

Energy-constrained Modulation Optimization

Shuguang Cui, *Member, IEEE*, Andrea J. Goldsmith, *Fellow, IEEE*,
and Ahmad Bahai, *Member, IEEE*

Abstract—We consider wireless systems where the nodes operate on batteries so that energy consumption must be minimized while satisfying given throughput and delay requirements. In this context, we analyze the best modulation strategy to minimize the total energy consumption required to send a given number of bits. The total energy consumption includes both the transmission energy and the circuit energy consumption. For uncoded systems, by optimizing the transmission time and the modulation parameters we show that up to 80% energy savings is achievable over non-optimized systems. For coded systems, we show that the benefit of coding varies with the transmission distance and the underlying modulation schemes.

Index Terms—Energy efficiency, modulation optimization, MQAM, MFSK.

I. INTRODUCTION

Recent hardware advances allow more signal processing functionality to be integrated into a single chip. It is believed that soon it will be possible to integrate an RF transceiver, A/D and D/A converters, baseband processors, and other application interfaces into one device that is as small as a coin and can be used as a fully-functional wireless node. Such wireless nodes typically operate with small batteries for which replacement, when possible, is very difficult and expensive. Thus, in many scenarios, the wireless nodes must operate without battery replacement for many years. Consequently, minimizing the energy consumption is a very important design consideration. In [1], the authors show that the hardware, the link layer, the MAC layer, and all other higher layers should be jointly designed to minimize the total energy consumption. The μ AMPs project [2] at MIT and the PicoRadio project [3] at Berkeley are investigating energy-constrained radios and their impact on overall network design.

Achieving an optimal joint design across all layers of the network protocol stack is quite challenging. We therefore consider pair-wise optimization of the hardware and link layer designs. We investigate the energy consumption associated with both the transmitting path and the receiving path: namely the total energy required to convey a given number of bits to the receiver for reliable detection. Assuming all nodes transmit and receive about the same amount of data, minimizing the

energy consumption along both the transmitting path and the receiving path at the same time is more appropriate than minimizing them separately.

The issue of energy saving is significant since in a wireless node, the battery energy is finite and hence a node can only transmit a finite number of bits. The maximum number of bits that can be sent is defined by the total battery energy divided by the required energy per bit. Most of the pioneering research in the area of energy-constrained communication has focused on transmission schemes to minimize the transmission energy per bit. In [4] the authors discuss some optimal strategies that minimize the energy per bit required for reliable transmission in the wide-band regime. In [5] the authors propose an optimal scheduling algorithm to minimize transmission energy by maximizing the transmission time for buffered packets. In [6] and [7], some other scheduling methods are proposed to minimize the transmission energy. The emphasis on minimizing transmission energy is reasonable in the traditional wireless link where the transmission distance is large (≥ 100 m), so that the transmission energy is dominant in the total energy consumption. However, in many recently-proposed wireless ad-hoc networks (*e.g.*, sensor networks) the nodes are densely distributed, and the average distance between nodes is usually below 10 m. In this scenario, the circuit energy consumption along the signal path becomes comparable to or even dominates the transmission energy in the total energy consumption. Thus, in order to find the optimal transmission scheme, the overall energy consumption including both transmission and circuit energy consumption needs to be considered. In [8], some insightful observations are drawn for choosing energy-efficient modulation schemes and multi-access protocols when both transmission energy and circuit energy consumption are considered. It is shown that M-ary modulation may enable energy savings over binary modulation for some short-range applications by decreasing the transmission time. In [10], uncoded MQAM modulation is analyzed in detail, and optimal strategies to minimize the total energy consumption are proposed for AWGN channels. In this work, we extend these ideas to a detailed tradeoff analysis of the transmission energy, the circuit energy consumption, the transmission time, and the constellation size for both uncoded and coded MQAM and MFSK in AWGN channels. This analysis also takes peak-power and delay constraints into account.

For both MQAM and MFSK we minimize the total energy consumption required to meet a given BER requirement by optimizing the transmission time. The transmission time is bounded above by the delay requirement and bounded below by the peak-power constraint. The transmission energy is analyzed via probability of error bound approximations and

Manuscript received July 27, 2003; revised March 5, 2004. This work was supported by the National Semiconductor Corporation, the Alfred P. Sloan Foundation, and the U.S. Army under MURI award W911NF-05-1-0246. Part of this work has been presented at ICC'03 and Globecom'03.

S. Cui is with the Dept. of Electrical and Computer Engineering, University of Arizona, Tucson, AZ, 85721 (email: cui@ece.arizona.edu).

A. J. Goldsmith is with the Wireless System Lab, Dept. of Electrical Engineering, Stanford University, Stanford, CA, 94305 (email: andrea@wsl.stanford.edu).

A. Bahai is with National Semiconductor, Santa Clara, CA, 95051, and he is also a consulting professor at Stanford University, Stanford, CA, 94305 (email: bahai@stanford.edu).

the circuit energy consumption is approximated as a linear function of the transmission time. From this optimization, we also find the optimal constellation size for MQAM and for MFSK. The effects of coding is modeled by the coding gain and the corresponding bandwidth expansion wherever applicable. For MQAM, trellis-coded modulation is studied for the energy minimization problem. For MFSK, a convolutionally coded system is discussed, where we show that the benefits of coding varies with the transmission distance.

The remainder of this paper is organized as follows. Section II describes the system model. Section III solves the energy-constrained modulation problem for uncoded MQAM and MFSK, respectively. In Section IV, the energy-minimization problem for coded MQAM and MFSK is discussed. Section V discusses the optimization algorithms. Section VI makes some comments on the possible extension to the multiple access scenario. Section VII summarizes our conclusions. Power estimation models for various circuit blocks are discussed in the appendix.

II. SYSTEM MODEL

We consider a communication link connecting two wireless nodes. In order to minimize the total energy consumption, all signal processing blocks at the transmitter and the receiver need to be considered in the optimization model. However, for typical energy-constrained wireless networks such as sensor networks, the throughput requirement is usually low such that the baseband symbol rate is low. We also assume that no complicated signal processing techniques such as multi-user detection or iterative decoding are used. Thus, the power consumption in the baseband is mainly defined by the symbol rate and the complexity of the digital logic. This power consumption is quite small [9] compared with the power consumption in the RF circuitry, which is closely related to the carrier frequency. Thus, at this stage we neglect the energy consumption of baseband signal processing blocks (e.g., source coding, pulse-shaping, and digital modulation) to simplify the model. The resulting signal paths on the transmitter and receiver sides are shown in Fig. 1, where we see that on the transmitter side the baseband signal is first converted to an analog signal by the Digital-to-Analog Converter (DAC), then filtered by the low-pass filter and modulated by the mixer, then filtered again, and finally amplified by the Power Amplifier (PA) and transmitted to the wireless channel. On the receiver side the RF signal is first filtered and amplified by the Low Noise Amplifier (LNA), then cleaned by the anti-aliasing filter and down-converted by the mixer, then filtered again before going through the Intermediate Frequency Amplifier (IFA) whose gain is adjustable, and finally converted back to a digital signal via the Analog-to-Digital Converter (ADC). The last-stage demodulation is done digitally. Although this model is based on a generic low-IF transceiver structure, our framework can be easily modified to analyze other architectures as well.

We assume that the transceiver circuitry works on a multi-mode basis: when there is a signal to transmit all circuits work in active mode, when there is no signal to transmit they work in sleep mode, and when switching from sleep mode to active

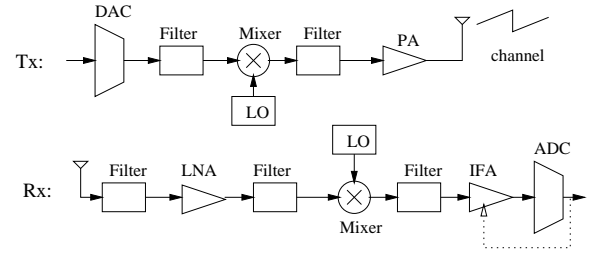


Fig. 1. Transceiver Circuit Blocks (Analog)

mode there is a transient mode. The multi-mode operation provides a significant savings of energy when the sleep mode is deployed.

We assume that a node has L bits to transmit with a deadline T . This setup can be justified in a typical sensor network where each sensor periodically takes measurements, encodes these measurements into a certain number of bits, and transmits them to a central processor. The measurements must arrive at the processor in a timely manner for effective processing. In this scenario, the transceiver spends time $T_{on} \leq T$ to communicate these bits, where T_{on} is a parameter to optimize, and then returns to the sleep mode where all the circuits in the signal path are shut down for energy saving. Although the transient duration from active mode to sleep mode is short enough to be negligible, the start-up process from sleep mode to active mode may be slow due to the finite Phase Lock Loop (PLL) settling time in the frequency synthesizer. Thus, the transmission period T is given by $T = T_{tr} + T_{on} + T_{sp}$, where T_{tr} is the transient mode duration which is equal to the frequency synthesizer settling time (the start-up process of the mixer and power amplifier is fast enough to be neglected) and T_{sp} is the sleep mode duration. Correspondingly, the total energy consumption E required to send L bits also consists of three components:

$$\begin{aligned} E &= P_{on}T_{on} + P_{sp}T_{sp} + P_{tr}T_{tr} \\ &= (P_t + P_{c0})T_{on} + P_{sp}T_{sp} + P_{tr}T_{tr}, \end{aligned} \quad (1)$$

where P_{on} , P_{sp} and P_{tr} are power consumption values for the active mode, the sleep mode, and the transient mode, respectively. The active mode power P_{on} comprises the transmission signal power P_t and the circuit power consumption P_{c0} in the whole signal path. Specifically, P_{c0} consists of the mixer power consumption P_{mix} , the frequency synthesizer power consumption P_{syn} , the LNA power consumption P_{LNA} , the active filter power consumption P_{filt} at the transmitter, the active filter power consumption P_{filt} at the receiver, the IFA power consumption P_{IFA} , the DAC power consumption P_{DAC} , the ADC power consumption P_{ADC} , and the power amplifier power consumption P_{amp} , where $P_{amp} = \alpha P_t$ and $\alpha = \frac{\xi}{\eta} - 1$ with η the drain efficiency [11] of the RF power amplifier and ξ the Peak to Average Ratio (PAR), which is dependent on the modulation scheme and the associated constellation size. Although strictly speaking P_t should be part of the total amplifier power consumption, here we define P_{amp} as the value excluding the transmission signal power for convenience. The calculation of P_{IFA} , P_{ADC} and P_{DAC} is

based on the model introduced in the appendix.

Since batteries are not only energy-limited but also peak-power-limited, the total power consumption of either the transmitter or the receiver can never exceed the maximum available battery power. The maximum power available for the transmitter signal path is denoted as $P_{max,t}$, which is equal to the maximum battery output power at the transmitting node minus the total power consumption in all other circuits inside the same node. The maximum power available for the receiver signal path $P_{max,r}$ is defined in the same manner. Since $P_{on} = \max\{P_{on}, P_{tr}, P_{sp}\}$, the peak-power constraints are given by

$$\begin{aligned} P_{ont} &= P_t + P_{amp} + P_{ct} = (1 + \alpha)P_t + P_{ct} \leq P_{max,t} \\ P_{onr} &= P_{cr} \leq P_{max,r} \end{aligned} \quad (2)$$

where P_{ont} is the value of P_{on} at the transmitter and P_{onr} is the value of P_{on} at the receiver. Meanwhile, $P_{ct} = P_{mix} + P_{syn} + P_{filt} + P_{DAC}$ and $P_{cr} = P_{mix} + P_{syn} + P_{LNA} + P_{filr} + P_{IFA} + P_{ADC}$ denote the circuit power consumption (excluding the power amplifier power consumption) in the active mode at the transmitter and the receiver, respectively. In the following sections $P_c T_{on} = (P_{ct} + P_{cr})T_{on}$ will be used to denote the total circuit energy consumption.

The start-up time for other circuit blocks is negligible compared to that of the frequency synthesizers. Hence, the optimal strategy for the start-up process is to turn on the frequency synthesizers first and once they settle down, to turn on the rest of the circuits. As a result, there is no energy wasted while the transceiver waits for the frequency synthesizers to settle down. Hence, P_{tr} merely needs to include the power consumption of the frequency synthesizers.

In the sleep mode, the power consumption is dominated by the leaking current I_l of the switching transistors if the circuitry is properly designed. Since the leaking power consumption is usually much smaller than the power consumption in the active mode (which may not be true for deep sub-micron CMOS technology [11]), it is neglected in our model. Thus, we set $P_{sp} = 0$. Our analysis can be easily modified to incorporate $P_{sp} \neq 0$.

Given Eq. (1) and Eq. (2), and the fact that $P_{sp} = 0$ and $P_{tr} \approx 2P_{syn}$, the energy consumption per information bit $E_a = E/L$ is given by

$$\begin{aligned} E_a &= (((1 + \alpha)P_t + P_c)T_{on} + P_{tr}T_{tr})/L \\ &\approx ((1 + \alpha)E_t + P_c T_{on} + 2P_{syn}T_{tr})/L, \end{aligned} \quad (3)$$

where $E_t = P_t T_{on}$, and P_c , P_{syn} and T_{tr} can be treated as constants defined by the particular transceiver structure in use. It can be shown [12] that the transmission energy E_t is a monotonically increasing function of the bandwidth efficiency defined as $B_e = L/(BT_{on})$ (in bits/s/Hz). In other words, E_t is a monotonically decreasing function of T_{on} for any fixed packet size L and bandwidth B .

One thing we need to point out is that since the model shown in Fig. 1 is a generic model, it may need some modifications for specific systems. For example, the mixer and the DAC at the transmitter side are not needed for MFSK systems since frequency modulation is usually implemented digitally

inside the frequency synthesizer. As a result, for MFSK the P_c term in all the energy consumption formulas should exclude the energy terms related to the mixer and the DAC on the transmitter side.

Finally, the energy-constrained modulation problem can be modeled as

$$\begin{aligned} &\text{minimize} && E_a \\ &\text{subject to} && 0 \leq T_{on} \leq T - T_{tr} \\ &&& 0 \leq (1 + \alpha)P_t + P_{ct} \leq P_{max,t} \end{aligned} \quad (4)$$

where we see that our task is to find the most efficient way to choose the transmission time under the given system constraints so that the total energy consumption is minimized. For the two constraints, the first one corresponds to the delay constraint and the second one corresponds to the peak-power constraints. Since P_{cr} is independent of the design variables, the constraint $0 \leq P_{cr} \leq P_{max,r}$ is not included in the optimization model and we assume that it is satisfied by default. From the resulting optimal T_{on} , the optimal constellation size for a particular modulation scheme can be obtained.

III. UNCODED MQAM AND MFSK

A. Uncoded MQAM

We first take MQAM as a design example. Analysis is done over an AWGN channel. For MQAM, the number of bits per symbol is defined as $b = \log_2 M$. The number of MQAM symbols needed to send L bits is denoted as $L_s = \frac{L}{b}$. If the symbol period is denoted as T_s , we can also represent L_s as $L_s = \frac{T_{on}}{T_s}$. Thus, $\frac{L}{b} = \frac{T_{on}}{T_s}$, i.e.,

$$b = \frac{LT_s}{T_{on}}. \quad (5)$$

If square pulses are used and $T_s \approx 1/B$ is assumed, we have

$$b \approx \frac{L}{BT_{on}}. \quad (6)$$

Since the bandwidth efficiency is defined as $B_e = \frac{L}{BT_{on}}$, we can see that $b \approx B_e$ for MQAM.

A bound on the probability of bit error for MQAM is given by [13]

$$P_b \leq \frac{4}{b} \left(1 - \frac{1}{\sqrt{2^b}}\right) Q\left(\sqrt{\frac{3}{2^b - 1}} \gamma\right) \leq \frac{4}{b} \left(1 - \frac{1}{\sqrt{2^b}}\right) e^{-\frac{3}{2^b - 1} \frac{\gamma}{2}},$$

where $Q(x) = \int_x^\infty \frac{1}{\sqrt{2\pi}} e^{-\frac{u^2}{2}} du$. The Signal to Noise Ratio (SNR) γ is defined as $\gamma = \frac{P_r}{2B\sigma^2 N_f}$, where P_r is the received signal power, σ^2 is the power spectral density of the AWGN and N_f is the receiver noise figure defined as $N_f = \frac{N_{total}}{2B\sigma^2}$, where N_{total} is the power of the noise introduced by the receiver front-end.

Hence, by approximating the bound as an equality we obtain

$$P_r \approx \frac{4}{3} N_f B \sigma^2 (2^b - 1) \ln \frac{4(1 - \frac{1}{\sqrt{2^b}})}{b P_b}. \quad (7)$$

Assuming a κ^{th} -power path-loss model at distance d (meters), the transmission power is equal to

$$P_t = P_r G_d, \quad (8)$$

where $G_d \triangleq G_1 d^\kappa M_l$ is the power gain factor with M_l the link margin compensating the hardware process variations and other additive background noise or interference and G_1 the gain factor at $d = 1$ m which is defined by the antenna gain, carrier frequency and other system parameters. We will assume $\kappa = 3.5$ and $G_1 = 30$ dB for our model [18]. According to Eqns. (6)–(8), we obtain the transmission energy as

$$\begin{aligned} E_t &= P_t T_{on} \\ &\approx \frac{4}{3} N_f \sigma^2 (2^{\frac{L}{BT_{on}}} - 1) \ln \frac{4(1 - 2^{-\frac{L}{2BT_{on}}})}{\frac{L}{BT_{on}} P_b} G_d B T_{on}. \end{aligned} \quad (9)$$

It is easily shown that E_t is a monotonically decreasing function over the product BT_{on} when MQAM is well defined, i.e., when $b = \frac{L}{BT_{on}} \geq 2$. Thus, when the packet size L and bandwidth B are fixed, the maximum allowable T_{on} minimizes the transmission energy.

However, when we include the circuit energy consumption in the model, the situation may change. According to Eq. (3), the expression for the total energy consumption per information bit in terms of T_{on} is given by

$$\begin{aligned} E_a &= ((1 + \alpha) \frac{4}{3} N_f \sigma^2 (2^{\frac{L}{BT_{on}}} - 1) \ln \frac{4(1 - 2^{-\frac{L}{2BT_{on}}})}{\frac{L}{BT_{on}} P_b} \\ &\quad \times G_d B T_{on} + P_c T_{on} + 2P_{syn} T_{tr}) / L, \end{aligned} \quad (10)$$

where $\alpha = \frac{\xi}{\eta} - 1$ is also a function of T_{on} since for MQAM $\xi = 3 \frac{\sqrt{M}-1}{\sqrt{M+1}}$ and $M = 2^{\frac{L}{BT_{on}}}$ (a square constellation is assumed [14]).

From the expression for E_a we see that the maximum T_{on} minimizes the transmission energy while the minimum T_{on} minimizes the circuit energy consumption. Therefore, an optimal tradeoff for T_{on} needs to be found to minimize the total energy consumption. In addition, the value for T_{on} needs to be optimized under the delay and peak-power constraints. The peak-power constraint in Eq. (4) can be rewritten as

$$\begin{aligned} (1 + \alpha) \frac{4}{3} N_f \sigma^2 (2^{\frac{L}{BT_{on}}} - 1) \ln \frac{4(1 - 2^{-\frac{L}{2BT_{on}}})}{\frac{L}{BT_{on}} P_b} G_d B \\ \leq P_{max} - P_{ct}, \end{aligned} \quad (11)$$

which is equivalent to

$$T_{on} \geq T_{min}, \quad (12)$$

where T_{min} is the solution for T_{on} for which the equality in Eq. (11) holds. Thus, for MQAM the optimization model in Eq. (4) can be rewritten as

$$\begin{aligned} &\text{minimize } E_a \\ &\text{subject to } T_{min} \leq T_{on} \leq T - T_{tr}. \end{aligned} \quad (13)$$

If we take into account the fact that $b = \frac{L}{BT_{on}}$, an equivalent representation for the optimization model can be written as follows

$$\begin{aligned} &\text{minimize } E_a \\ &\text{subject to } b_{min} \leq b \leq b_{max}, \end{aligned} \quad (14)$$

where the upper bound on b corresponds to the lower bound on T_{on} given by $b_{max} = \lfloor \frac{L}{BT_{min}} \rfloor$, the lower bound on b is

TABLE I
MQAM PARAMETERS

$f_c = 2.5$ GHz	$\eta = 0.35$
$\kappa = 3.5$	$\sigma^2 = \frac{N_0}{2} = -174$ dBm/Hz
$B = 10$ KHz	$L = 2$ kb
$P_{mix} = 30.3$ mW	$P_{syn} = 50$ mW
$P_{LNA} = 20$ mW	$P_{IFA} = 3$ mW
$P_{max} = 250$ mW	$P_{filt} = P_{filr} = 2.5$ mW
$T_{tr} = 5$ μ s	$M_l = 40$ dB
$T = 100$ ms	$P_b = 10^{-3}$
$N_f = 10$ dB	$G_1 = 30$ dB

given by $b_{min} = \max\{\lceil \frac{L}{B(T-T_{tr})} \rceil, 2\}$, and E_a is represented in terms of b as

$$\begin{aligned} E_a &= (1 + \alpha) \frac{4}{3} N_f \sigma^2 \frac{(2^b - 1)}{b} \ln \frac{4(1 - 2^{-\frac{b}{2}})}{b P_b} \\ &\quad \times G_d + (P_c T_{on} + 2P_{syn} T_{tr}) / L. \end{aligned} \quad (15)$$

The resulting optimization problem can be solved using the optimization algorithms discussed in Section V.

For a specific numerical example, the circuit-related parameters need to be defined first. We take a 2.5 GHz radio in the Industrial-Scientific-Medical (ISM) band as an example. For radios in other bands or with significantly different hardware architectures we need to use different parameters. The circuitry for such a radio is composed of several blocks described in [11], [15], [16], and [17]. The corresponding parameters are summarized in Table I, where $\eta = 0.35$, which is a practical value for class-A RF power amplifiers [11] (Due to the linearity requirement for amplifying MQAM signals, class-A power amplifiers are usually used.). The values for B , L , and T are set up such that $b_{min} = \frac{L}{BT} = 2$. Thus, the constellation size for MQAM is well defined inside the feasible region.

The plot of E_a over T_{on} for bandwidth $B = 10$ KHz is shown in Fig. 2. The vertical axis is the energy consumption per information bit (in terms of dB relative to a millijoule: $\log_{10} \frac{E_a}{0.001}$ dBmJ). The horizontal axis is the normalized transmission time. We see that the total energy consumption is not a monotonically-decreasing function of T_{on} when the transmission distance d is small. For example, when $d = 1$ m, E_a at the optimal $T_{on}^* \approx 0.12T$ is about 8 dB lower than the non-optimized case where $T_{on} = T - T_{tr} \approx T$. Thus, T_{on} optimization results in an 84% energy saving. It can be shown that when $d = 100$ m, the peak-power constraint is violated even when $b = 2$ (the minimum allowable value). In this case, we can use coding or MFSK modulation to reduce the peak power requirement, as we show later.

The transmission energy is dependent on the transmission distance d while obviously the circuit energy consumption is independent of d . Thus, we can save energy by optimizing T_{on} only when the circuit energy consumption is nontrivial relative to the transmission energy. Since the transmission energy increases with d , there exists a threshold for the value of d above which there is no energy savings possible by optimizing T_{on} , which then should just be set to the maximum value T . For the above example, $d = 30$ m is the threshold, where the derivative of E_a relative to T_{on} is approximately zero at the point $T_{on}/T \approx 1$. In general, to find the threshold

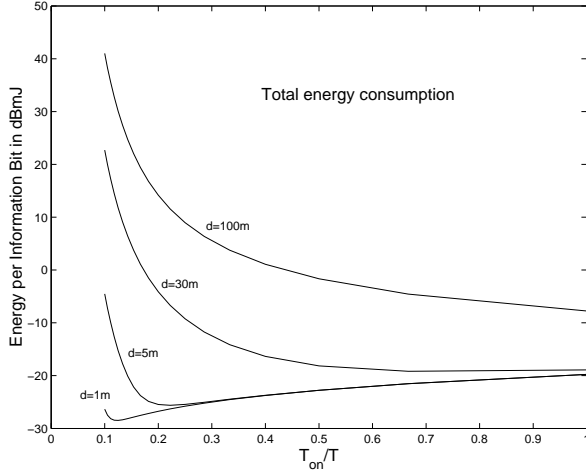


Fig. 2. Total Energy Consumption, MQAM, (AWGN)

we just need to find the value of d that makes the derivative of E_a relative to T_{on} at the maximum transmission time equal to zero.

According to the relationship defined in Eq. (6), we can find the optimal constellation size from the optimal value of T_{on} . We redraw E_a over b for the $d = 5$ m case in Fig. 3. We see from the figure that $b_{opt} \approx 9$ if the total energy consumption is considered versus $b_{opt} = 2$, its minimum value, when only transmission energy is considered.

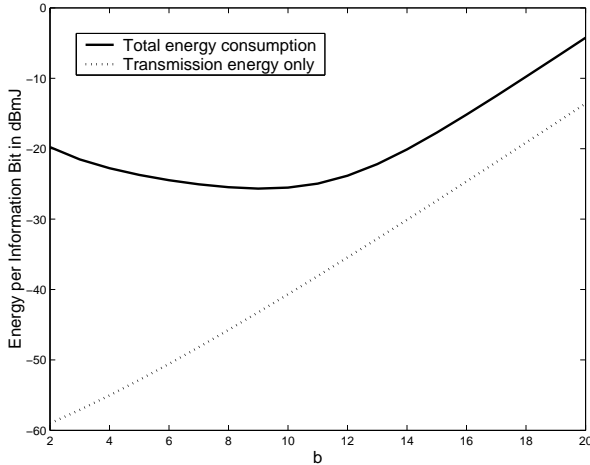


Fig. 3. Total energy consumption versus constellation size, MQAM (AWGN)

B. Uncoded MFSK

For MFSK, the number of orthogonal carriers is $M = 2^b$. We assume that the carrier separation is equal to $\frac{1}{2T_s}$, where T_s is the symbol period. Thus, the data rate $R = \frac{b}{T_s}$ and the total bandwidth can be approximated as $B \approx \frac{2^b}{2T_s}$ (see [13]). As a result, the bandwidth efficiency for MFSK is given by

$$B_e \triangleq 2b/2^b \quad (b/s/Hz). \quad (16)$$

Since in general the bandwidth efficiency can also be represented as $B_e = \frac{L}{BT_{on}}$ regardless of modulation schemes, the

relationship between the constellation size and the bandwidth-time product for MFSK is given by

$$2b/2^b = L/(BT_{on}), \quad (17)$$

which is different from the MQAM case where $b = L/(BT_{on})$. However, there still exists a one-to-one relationship between b and the BT_{on} product for any fixed value of L , except for $b = 1$ and $b = 2$, which correspond to the same BT_{on} product. For simplicity, all the following transmission energy functions for MFSK will be represented in term of b .

Since most practical MFSK receivers use non-coherent detectors, the probability of error bound for non-coherent MFSK detection is used in our derivation:

$$P_b \leq 2^{b-2} e^{-\frac{\gamma}{2}}. \quad (18)$$

Approximating the bound as an equality, we obtain $\gamma = \frac{bE_b}{N_0N_f} \approx 2 \ln \frac{2^{b-2}}{P_b}$, where E_b is the energy per information bit at the receiver and $N_0 = 2\sigma^2$. Hence, $\frac{E_b}{2\sigma^2N_f} = \frac{2}{b} \ln \frac{2^{b-2}}{P_b}$. Following a similar derivation as in the MQAM case, the transmission power and the transmission energy are given by

$$P_t = 4N_f\sigma^2 \ln \frac{2^{b-2}}{P_b} G_d \frac{2B}{2^b} \quad (19)$$

and

$$E_t = P_t T_{on} = 4N_f\sigma^2 \ln \frac{2^{b-2}}{P_b} G_d \frac{L}{b} \quad (20)$$

respectively, where we used $T_{on} = \frac{2^b L}{2b B}$ derived from Eq. (17).

One necessary modification in the hardware configuration of MFSK compared to the MQAM system is that the mixer and the DAC at the transmitter should be deleted, as we discussed earlier. Correspondingly we redefine $P_c = 2P_{syn} + P_{mix} + P_{LNA} + P_{filt} + P_{filr} + P_{IFA} + P_{ADC}$. Thus, the total energy consumption per information bit is given by

$$E_a = \left((1 + \alpha) 4N_f\sigma^2 \ln \frac{2^{b-2}}{P_b} G_d \frac{L}{b} + P_c T_{on} + 2P_{syn} T_{tr} \right) / L, \quad (21)$$

where $\alpha = \frac{\xi}{\eta} - 1$ and $\xi = 1$ for MFSK. From Eq. (17) we see that the product of B and T_{on} defines the value of b when the packet size L is fixed. Hence, the value of E_t is dependent on the BT_{on} product. It can be proved that E_t is a monotonically decreasing function over b (when $b \geq 1$) unless P_e is unreasonably large (on the order of 0.1). Due to the relationship between b and BT_{on} as described in Eq. (17), E_t is also a monotonically decreasing function over the BT_{on} product which is similar to the MQAM case. Hence, increasing T_{on} always decreases the transmission energy, but the optimal T_{on} which minimizes the total energy consumption may not be the maximum allowable transmission time. The optimization model is easily described in term of b such that Eq. (4) can be rewritten as

$$\begin{aligned} & \text{minimize} && E_a \\ & \text{subject to} && b_{min} \leq b \leq b_{max} \end{aligned} \quad (22)$$

where b_{max} is defined by the delay requirement in such a way that $\frac{2b_{max}}{2^{b_{max}}} = \frac{L}{BT}$ and b_{min} is calculated based on the peak-power constraint, specifically, $(1 + \alpha)P_t(b_{min}) = P_{max} - P_{ct}$ where $P_{ct} = P_{syn} + P_{filt}$.

To give a numerical example, we first assume that the power consumption of the corresponding circuit blocks is roughly the same as in the MQAM case. Since there is no longer a strict linearity requirement on the RF power amplifier, the value of η in Table I is changed to 0.75, which corresponds to a class-B or a higher-class (C,D or E) power amplifier. The bandwidth B and the packet size L are kept as 10 KHz and 2 Kb, respectively. The maximum delay T is changed to 1.07 s, such that $b_{max} = 6$. Compared with the MQAM case, the increase of T is due to the fact that MFSK is less bandwidth-efficient than MQAM. Thus, MFSK needs a longer transmission time to transmit the same number of bits as MQAM when they have the same bandwidth.

We draw E_t and E_a directly over b as shown in Fig. 4. Not surprisingly, the transmission energy E_t goes down when b increases, since it is well known that the larger M is, the more energy-efficient MFSK is, in an AWGN channel. In other words, $M = \infty$ is optimal in the sense of minimizing the energy consumption per information bit [13] based only on transmission energy. When the circuit energy consumption is considered, as shown in Fig. 4, $b = 2$ turns out to be the best choice for both $d = 1$ m and $d = 30$ m. For the $b = 1$ m case, by using $b_{opt} = 2$ we can achieve about 80% energy savings when compared with the case where $b = 6$ ($T_{on} = T$) is used.

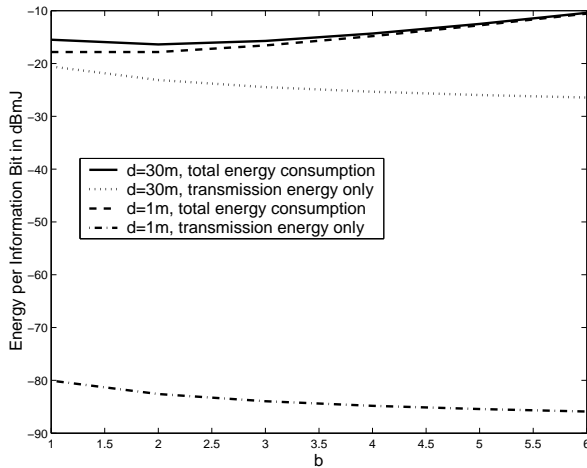


Fig. 4. Total energy consumption versus b , MFSK (AWGN)

IV. CODED MQAM AND MFSK

It is well known [13] that forward Error Correction Codes (ECCs) can reduce the required value of E_b/N_0 to meet a given target probability of bit error P_b , where E_b refers to the received energy per information bit, which is proportional to the transmission energy per information bit. However, whether the total energy consumption per information bit can be reduced is not clear due to the possible bandwidth expansion caused by the ECC redundancy and the extra baseband energy consumption of the ECC codec.

The error-correction capability of ECCs is enabled by introducing controlled redundancy, which usually causes bandwidth expansion in order to communicate the extra redundant bits. If the bandwidth expansion in the frequency domain is not

limited, the system throughput can be maintained by increasing the symbol rate. However, most practical systems are assigned a fixed frequency band so that the bandwidth expansion can only be implemented in the time domain. In other words, a longer transmission time is needed in order to communicate both the information bits and the error-correction bits. Whether the expansion happens in the time domain or in the frequency domain has no impact on the ECC performance as the coding gain remains the same. Nevertheless, the time domain approach results in more circuit energy consumption which is linearly proportional to the increase of transmission time T_{on} . Fortunately, bandwidth expansion may be circumvented when the channel coding and modulation processes are jointly designed, for example in trellis-coded MQAM [13].

In the following sections we consider two coded systems: trellis-coded MQAM and convolutionally-encoded MFSK. For trellis-coded MQAM, even though there is no bandwidth expansion, there is still an energy penalty caused by the baseband ECC processing. We first neglect this energy penalty due to its small magnitude compared with the energy consumption of the RF circuitry and then show its effect with an example where the transmission distance is extremely small. Therefore, it will be shown in the next section that trellis-coded MQAM always has higher energy efficiency than uncoded MQAM for narrow-band systems. For MFSK systems with fixed bandwidth, we cannot implement coding by increasing the constellation size while keeping the transmission time constant, as we do in trellis-coded MQAM. In other words, bandwidth expansion is inevitable for coded MFSK. We will therefore investigate the tradeoff between energy savings and bandwidth expansion for MFSK systems with convolutional codes.

A. Coded MQAM

In a trellis-coded MQAM system, each block (of size b) of information bits is divided into two groups of size b_1 and b_2 , respectively. The first group of b_1 bits is convolutionally encoded into b_k bits, which map to 2^{b_k} constellation subsets. The second group of b_2 bits are used to choose the 2^{b_2} th constellation point within each subset (see [13] for a detailed description of trellis-coded modulation). The code rate is therefore defined as $\gamma_c = b_1/b_k$ and the constellation size is increased from 2^b to $2^{b_k+b_2}$. A rate $\gamma_c = b_1/(b_1 + 1)$ code is usually used for subset selection. According to [13], $b_1 = 2$ is a good choice since it provides the major part of the achievable coding gain. In our model, a rate 2/3 code with 32 states is chosen and the coding gain $G_c \approx 3$ (4.7 dB) [13]. As the result, the final constellation size becomes 2^{b_c} , where $b_c = 1 + \frac{L}{BT_{on}}$.

Due to the embedded ECC, the required SNR threshold γ_0 to achieve a given P_b is reduced by the coding gain G_c , i.e., for any $b = \frac{L}{BT_{on}}$, $\gamma_0 = \frac{E_b b}{G_c N_0}$. Therefore, for trellis-coded MQAM the required transmission energy to achieve a given P_b is changed to $E_{tc} = E_t/G_c$ and the total energy consumption E_{ac} is given as

$$E_{ac} = (1 + \alpha) \frac{4}{3G_c} N_f \sigma^2 \frac{(2^b - 1)}{b} \ln \frac{4(1 - 2^{-\frac{b}{2}})}{bP_b} \times G_d + (P_c T_{on} + 2P_{syn} T_{tr})/L. \quad (23)$$

For a specific numerical example, the circuit-related parameters are the same as in the uncoded case (see Table I). The values for B , L , and T are set up in such a way that $b_{min} = \frac{L}{BT} = 2$ for an uncoded system. Thus, for the trellis-coded system in our model, the minimum value for b_c will be equal to 3. For comparison, an optimized uncoded system is also considered. We also evaluate one reference uncoded system with constellation size $b = 2$ and one reference coded system with constellation size $b_c = 3$: these reference systems are designed to minimize the transmission energy.

The plots of minimized energy per information bit over different transmission distances are shown in Fig. 5, where we see that about 90% energy savings is achieved over the reference setup for the coded system when $d = 1$ m. The plots also show that for both the coded and uncoded systems, the optimized performance converges to be the same as the reference performance when the transmission distance is large. In other words, optimizing over modulation parameters no longer saves energy at large distances, since in this case transmission energy is dominant and therefore using the minimum allowable constellation size is always optimal. We also see that the coded system outperforms the uncoded system over all the distances (when ECC processing energy is not included).

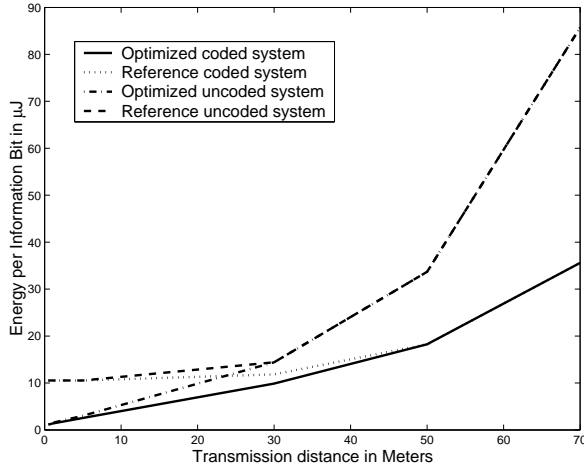


Fig. 5. Total Energy Consumption per Information Bit v.s. Distance, MQAM

The optimized parameters are listed in Table II, where b_{opt} is the optimal constellation size, E is the total energy consumption per information bit, E_{ref} is the corresponding energy consumption for the reference systems, and each item x/y inside the table has x as the optimized value for the coded system and y as the optimized value for the uncoded system. In this example the peak-power constraint ($P_{ont} \leq P_{max}$) is violated when $d \geq 50$ m for both the coded system and the uncoded system. In order to achieve the given P_b at these distances we would have to increase the power budget or use other coding strategies.

If we include the ECC processing energy in the total energy consumption, at very short transmission distances where the transmission energy is low, the savings on transmission energy enabled by the ECC may be less than the ECC processing energy, which is mainly contributed by the Viterbi decoder.

TABLE II
OPTIMIZED PARAMETERS FOR CODED/UNCODED MQAM

d (m)	0.5	1	5	30	50
B (KHz)	10/10	10/10	10/10	10/10	10/10
T_{on} (ms)	10/10.5	11.8/12.5	20/25	66.7/100	100/100
b_{opt}	20/19	17/16	10/8	3/2	2/2
P_{out} (mW)	1.6/2.4	2.3/3.5	5.3/4.1	20.8/27.1	54/162
P_{ont} (mW)	112/119	118/128	141/129	183/176	253/561
P_{onr} (mW)	113/121	113/121	113/121	113/121	113/121
E (μ J)	1.1/1.2	1.4/1.5	2.5/3.0	9.9/14.4	18.3/33.7
E_{ref} (μ J)	10.5/10.5	10.5/10.5	10.5/10.5	11.8/14.4	18.3/33.7

In our example, since the symbol rate is as low as 10 KHz, the power consumption of the Viterbi decoder is only on the level of microwatts. Therefore, it is safe to say that the coded MQAM is always better than uncoded MQAM at practical transmission distances. When the bandwidth gets larger, the power consumption of the Viterbi decoder also becomes higher. As a result, uncoded MQAM may beat coded MQAM in terms of energy efficiency at short distances. For example, when $B = 10$ MHz and $L = 2$ Mb with all other parameters kept the same, the power consumption of the Viterbi decoder is around 10 mW. Thus, the uncoded system may become more energy-efficient than the coded one at short distances. As shown in Fig. 6, the reference uncoded system becomes more energy-efficient than the reference coded system when $d \leq 1.5$ m. For optimized systems, since higher constellation sizes reduce the transmission time, the energy consumption in the Viterbi decoder is compensated by the reduced energy consumption in the analog circuits. Therefore, the effect of the decoding process is not obvious. In other words, adaptive modulation is able to keep the superiority of coded systems down to a very short distance, as shown in the figure where the crossover happens at 0.1 m.

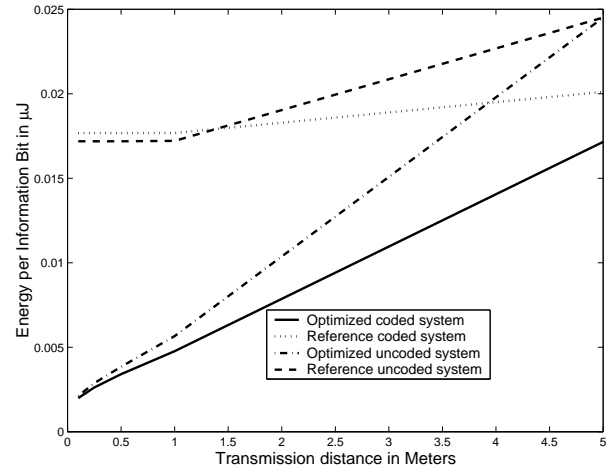


Fig. 6. Total Energy Consumption per Information Bit v.s. Distance, MQAM (ECC processing energy included)

For trellis-coded MQAM, the coding gain is more sensitive to the constraint length of the convolutional encoder than to the code rates. Codes with lower rates may not necessarily generate higher coding gain. Since there is no bandwidth expansion, any codes with higher coding gain are able to reduce the total energy consumption unless the constraint length is so large that the energy consumption in the decoding logic can no longer be neglected. The tradeoff between energy

consumption and code rates is complicated and definitely worth further investigation. However, this extension is beyond the scope of this paper.

B. Coded MFSK

For the coded MFSK system, we assume a rate $\gamma_c = 2/3$ convolutional code with 32 states, which achieves a coding gain $G_c = 2.6$ (4.2 dB) [13]. Since the available frequency band is fixed, the error-control bits are accommodated by bandwidth expansion in the time domain. Thus, the required transmission energy per information bit for coded systems is reduced by G_c at a price of increased transmission time $T_{onc} = T_{on}/\gamma_c$. The total energy consumption per information bit for the coded system is therefore given by

$$E_{ac} = (1 + \alpha)4N_f\sigma^2 \ln \frac{2^{b-2}}{P_b} G_d \frac{1}{bG_c} + (P_c T_{onc} + 2P_{syn} T_{tr})/L. \quad (24)$$

To give a numerical example, we first assume that the power consumption of the different circuit blocks for MFSK is roughly the same as the corresponding blocks for MQAM. Similar to the uncoded case, the drain efficiency is changed to $\eta = .75$, which corresponds to a class-B or a higher-class (C,D or E) power amplifier. The bandwidth B and the packet size L are kept as 10 KHz and 2 kb, respectively. Due to the coding, the delay constraint is increased to $1.07/\gamma_c = 1.61$ s for the coded system. For the purpose of comparison, one uncoded BFSK system and one coded BFSK system (with the same convolutional code) are set up as reference systems.

The total energy consumption per information bit over different transmission distances d is plotted in Fig. 7. This figure shows that optimizing over modulation parameters saves energy for both the coded and uncoded systems, and this energy saving increases with d . In addition, the uncoded system outperforms the coded system when d is small (< 48 m for the optimized cases). This is due to the fact that the ECC-enabled savings on transmission energy can no longer balance the extra circuit energy consumption caused by the increase in transmission time. The optimized parameters are listed in Table III. By comparing the energy consumption values in Table III and Table II, we see that although MFSK requires less transmission energy ($= P_t T_{on}$) than MQAM at the same distance, the total energy cost per information bit is higher for MFSK when d is small due to its high circuit energy consumption (T_{on} is larger for MFSK), as shown in Fig. 8. When d increases such that the transmission energy becomes dominant, MFSK becomes more energy-efficient than MQAM (at the price of using more transmission time). However, by comparing the energy consumption values for the coded and uncoded cases, we see that coding can increase the distance where MFSK beats MQAM in terms of energy efficiency.

V. OPTIMIZATION ALGORITHMS

Since the design variable b is defined over integer values, the corresponding optimization problem is a non-convex integer programming problem. Exhaustive search (which is used for the numerical examples in this paper) is a feasible way to

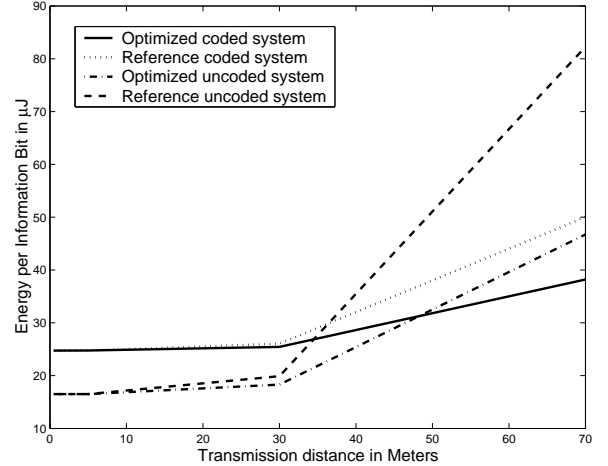


Fig. 7. Total Energy Consumption per Information Bit v.s. Distance, MFSK

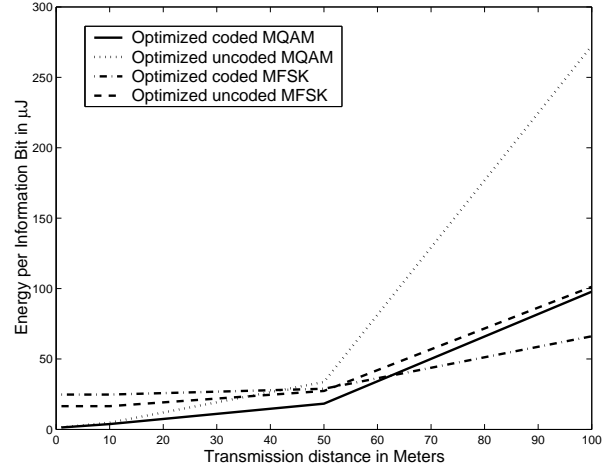


Fig. 8. Total Energy Consumption Comparison Between MQAM and MFSK

solve this problem for the simple point-to-point case, since only one variable is involved and all the constraints are well-bounded which makes the search algorithm relatively simple. However, we also investigated efficient algorithms to solve this type of integer programming problem. These algorithms can be used for example to extend the energy minimization results to multiple users [23]. Specifically, we found that if we use a looser bound on the total energy consumption per bit for MQAM, we are able to use an efficient convex relaxation method to solve this problem. For MFSK, even without using any looser bounds, the problem can be solved with efficient convex relaxation methods.

TABLE III
OPTIMIZED PARAMETERS FOR CODED/UNCODED MFSK

d (m)	0.5	1	5	30	70
B (KHz)	10/10	10/10	10/10	10/10	10/10
T_{on} (s)	0.3/0.2	0.3/0.2	0.3/0.2	0.3/0.2	0.3/0.27
b_{opt}	2/2	2/2	2/2	2/2	2/3
P_{out} (μ W)	0.002/0.008	0.02/0.09	6.5/25.6	3.5e3/1.4e4	6.7e4/1.4e5
P_{ont} (mW)	52.5/52.5	52.5/52.5	52.5/52.5	57.1/70.5	142/238
P_{onr} (mW)	112/112	112/112	112/112	112/112	112/112
E (μ J)	24.7/16.5	24.7/16.5	24.8/16.5	25.4/18.3	38.2/36.7
E_{ref} (μ J)	24.7/16.5	24.7/16.5	24.8/16.5	26/20	50/82.2

For uncoded MQAM, if we apply the bound $\ln \frac{4(1-2^{-\frac{b}{2}})}{bP_b} \leq \ln \frac{2}{P_b}$ for $b \geq 2$, we can simplify the representation for E_a as

$$E_a = x(1 + \alpha) \frac{2^b - 1}{b} L + y \frac{L}{b} + z, \quad (25)$$

with the coefficients x , y and z defined as

$$\begin{aligned} x &= \frac{4}{3} N_f \sigma^2 G_d \ln \frac{2}{P_b}, \\ y &= \frac{P_c}{B}, \\ z &= 2P_{syn} T_{tr}, \end{aligned} \quad (26)$$

respectively. The relative looseness caused by the bound $\ln \frac{4(1-2^{-\frac{b}{2}})}{bP_b} \leq \ln \frac{2}{P_b}$ is less than 21% when b is within the range $[2, 20]$ (which is a reasonable range for practical MQAM systems). If we relax b to be defined over real numbers, it can be proved that E_a is a convex function over b for $b \geq 2$ by showing that $\frac{\partial^2 E_a}{\partial b^2} \geq 0$. The optimization problem in Eq. (14) can then be rewritten as

$$\begin{aligned} &\text{minimize} && E_a \\ &\text{subject to} && b - b_{min} \geq 0 \\ &&& b_{max} - b \geq 0 \end{aligned} \quad (27)$$

Since all the constraints are simple linear constraints, the optimization problem is a convex problem, which can be efficiently solved using the interior point method [24]. Specifically, for a convex problem in the following format

$$\begin{aligned} &\text{minimize} && f_0(b) \\ &\text{subject to} && f_i(b) \geq 0 \quad i = 1, \dots, m \end{aligned} \quad (28)$$

we can first convert this constrained problem into an unconstrained one by utilizing the log-barrier functions [24]. The unconstrained problem is constructed as

$$\text{minimize} \quad t f_0(b) - \sum_{i=1}^m \ln(f_i(b)), \quad (29)$$

where $t > 0$ is a weighting factor. It has been shown [24] that for $\forall \epsilon > 0$, as $t > m/\epsilon$, the optimal solution for Eq. (29) is only ϵ away from the actual optimal solution for Eq. (28). The actual algorithm is given as follows:

Given a strictly feasible b_0 , $t := t_0 > 0$, step size $\mu > 1$, tolerance $\epsilon > 0$, we run

the Algorithm

- 1) Compute b^* by minimizing $t f_0(b) - \sum_{i=1}^m \ln(f_i(b))$, starting from b_0 .
- 2) Update: $b_0 = b^*$.
- 3) Quit if $m/t < \epsilon$.
- 4) Otherwise set $t = \mu t$ and go back to step 1).

For the algorithm to work, we first need to find a feasible point. Setting $b_0 = b_{max}$ is a natural choice. To make it strictly feasible [24], we can set $b_0 = b_{max} - \nu$, where ν is a small positive offset to drive b_0 away from the boundary. The unconstrained minimization problem in step 1) can be solved using standard numerical methods such as the Gaussian-Newton method [24].

After we find the optimal solution b^* for this relaxed optimization problem, we can find the optimal solution for

the original problem by evaluating E_a at the two neighboring integer points of b^* and choosing the one with smaller E_a . Note that for general integer programming problems defined over multiple integer variables, the optimal solution may not be one of the neighboring integer points surrounding the optimal solution for the relaxed convex problem.

For the coded MQAM, since E_a differs from that of the uncoded MQAM only by a constant G_c , the above algorithm can be directly applied to find the optimal solution. For both the uncoded and coded MFSK, we can show that a sufficient condition for the total energy consumption per bit to be convex over a relaxed b is given by $P_b \leq e^{-\frac{2}{\log_2 e}} = 0.25$, which can be easily satisfied by practical systems. Therefore, the above convex relaxation algorithm can also be applied directly to MFSK systems.

VI. MULTIPLE ACCESS SCENARIOS

Transmitting at higher rates as a result of adaptive modulation would create more interference to other users. Therefore, the results derived in this paper, which is based on pure MQAM and MFSK modulation schemes, cannot be directly extended to non-orthogonal multiple-access schemes. The possibility for combining the adaptive modulation with other multiple access coding schemes is currently under investigation. However, the adaptive modulation scheme proposed in this paper can be directly extended to orthogonal multiple access schemes such as TDMA. We propose such a variable-length energy-minimizing TDMA scheme in [23].

VII. CONCLUSIONS

We have shown that for transmitting a given number of bits in a point-to-point communication link, the traditional belief that a longer transmission duration lowers energy consumption may be misleading if the circuit energy consumption is included, especially for short-range applications. For both MQAM and MFSK, we show that the transmission energy is completely dependent on the product of B and T_{on} . To minimize the transmission energy, maximum transmission time is required. To minimize the total energy consumption, the transmission time needs to be optimized, where we show up to 80% energy savings is achievable via this optimization.

For trellis-coded narrow-band MQAM systems, we have shown that coding always increases energy efficiency, and the improvement increases with the transmission distance d . For MFSK systems, coding can only reduce energy consumption when the transmission distance is large such that the transmission energy is dominant. For short-range applications, uncoded MFSK outperforms coded MFSK due to the bandwidth expansion caused by ECC.

We found that uncoded MQAM is not only more bandwidth-efficient, but also more energy-efficient than uncoded MFSK for short-range applications. The performance difference is even more pronounced with coding. However, coded MFSK may be desirable in peak-power-limited applications since it requires less transmit power, although its total energy consumption may be higher.

ACKNOWLEDGMENT

The authors would like to thank Shwetabh Verma for helpful discussions on the hardware models.

APPENDIX

In the appendix, we discuss how to estimate the power consumption of various circuit blocks.

A. Power Consumption of DACs

We assume that a binary-weighted current-steering DAC is used [19]. The simplified diagram of the DAC is shown in Fig. 9.

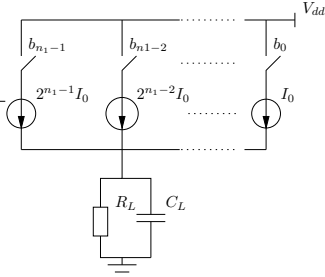


Fig. 9. Current-steering DAC

The power consumption consists of two components: static power consumption P_s and dynamic power consumption P_d . From Fig. 9 we see that the static power consumption is mainly contributed by the array of current sources and can be calculated as

$$P_s = V_{dd}I_0E\left[\sum_{i=0}^{n_1-1} 2^i b_i\right] = \frac{1}{2}V_{dd}I_0(2^{n_1} - 1), \quad (30)$$

where b_i 's are independent binary random variables and each has a probability of 1/2 to take 1 or 0, V_{dd} is the power supply and I_0 is the unit current source corresponding to the Least Significant Bit (LSB). The minimum possible value for I_0 is limited by the noise floor and device mismatch. Thus, for any given hardware technology we cannot decrease I_0 without bound to reduce the power consumption. The possible value for I_0 is also upper-bounded by the linearity requirement. However, since power consumption is the main concern in our design, I_0 will be set close to the lower bound.

The dynamic power consumption occurs during the switching process between symbols, *i.e.*, when the switch is being connected if the corresponding bit changes from 0 to 1 or when the switch is being disconnected if the corresponding bit changes from 1 to 0. For a first-order approximation, the average value for P_d can be calculated as $P_d \approx \frac{1}{2}n_1C_p f_s V_{dd}^2$, where C_p is the parasitic capacitance of each switch and the factor $\frac{1}{2}$ is the value of the switching factor (we assume that each switch has a probability of $\frac{1}{2}$ to change status during each symbol transition). For the low-IF structure assumed in our model, the sampling frequency can be approximately taken as $f_s = 2(2B + f_{cor})$, where f_{cor} is the corner frequency of the $1/f$ noise [11] and $f_{IF} = B + f_{cor}$ is the lowest possible value for IF such that the signal is not severely affected by

the $1/f$ noise. Thus, the expression for P_d can be rewritten as

$$P_d \approx n_1C_p(2B + f_{cor})V_{dd}^2. \quad (31)$$

As a result, the total power consumption of the DAC is given by

$$\begin{aligned} P_{DAC} &\approx \beta(P_s + P_d) \\ &\approx \beta\left(\frac{1}{2}V_{dd}I_0(2^{n_1} - 1) + n_1C_p(2B + f_{cor})V_{dd}^2\right), \end{aligned} \quad (32)$$

where β is a correcting factor to incorporate some second-order effects ($\beta = 1$ is used in our model).

B. Power Consumption of ADCs

We use the estimation model proposed in [20] for evaluating the power consumption of Nyquist-rate ADCs. As a result, the value of P_{ADC} can be calculated as follows

$$P_{ADC} \approx \frac{3V_{dd}^2 L_{min}(2B + f_{cor})}{10^{-0.1525n_2 + 4.838}}, \quad (33)$$

where L_{min} is the minimum channel length for the given CMOS technology.

C. Power Consumption of Viterbi Decoders

While the power consumption of a convolutional encoder is small enough to be neglected, the power consumption of a Viterbi decoder may be non-negligible in comparison with other receiver blocks. The model introduced in [21] is used to estimate the power consumption of Viterbi decoders.

D. Power Consumption of Other Blocks

We assume that the receiver gain adjustment is performed solely in the IFA. As a result, the power consumption values of the mixers, the frequency synthesizers, the filters, and the LNA can be approximated as constants and are quoted from several publications as we discussed earlier. For the IFA, its power consumption value is dependent on the receiver gain which varies along with the channel conditions. However, since P_{IFA} is usually much smaller than P_{syn} or P_{LNA} , we approximate P_{IFA} as a constant which is equal to 3 mW [22] in our model.

E. Parameter Setup

For the related parameters in our numerical examples, we take the following values: $V_{dd} = 3$ V, $L_{min} = 0.5$ μ m, $n_1 = n_2 = 10$, $f_{cor} = 1$ MHz, $I_0 = 10$ μ A, and $C_p = 1$ pF.

REFERENCES

- [1] A. J. Goldsmith and S. B. Wicker, "Design challenges for energy-constrained Ad Hoc wireless networks," *IEEE Wireless Communications Magazine*, pp. 8-27 Aug. 2002.
- [2] A. Chandrakasan, R. Amirtharajah, S. Cho, J. Goodman, G. Konduri, J. Kulik, W. Rabiner, and A. Y. Wang, "Design considerations for distributed microsensor systems," *Proc. IEEE CICC*, 1999.
- [3] J. Rabaey, J. Ammer, J. L. da Silva Jr., and D. Patel, "PicoRadio: Ad-hoc wireless networking of ubiquitous low-energy sensor/monitor nodes," *IEEE VLSI*, pp. 9-12, 2000.
- [4] S. Verdú, "Spectral efficiency in the wideband regime," *IEEE Trans. Information Theory*, vol. 48, pp. 1319-1343, June 2002.

- [5] A. E. Gamal, C. Nair, B. Prabhakar, E. Uysal-Biyikoglu and S. Zehedi, "Energy-efficient scheduling of packet transmissions over wireless networks," *Proc. IEEE Infocom*, 2002.
- [6] C. Schurgers, and M. B. Srivastava, "Energy efficient wireless scheduling: adaptive loading in time," *WCNC'02*, March, 2002.
- [7] P. Nuggehalli, V. Srinivasan, and R. R. Rao, "Delay constrained energy efficient transmission strategies for wireless devices," *INFOCOM'02*, June, 2002.
- [8] A. Y. Wang, S. Chao, C. G. Sodini, and A. P. Chandrakasan, "Energy efficient modulation and MAC for asymmetric RF microsensor system," *International Symposium on Low Power Electronics and Design*, pp. 106-111, 2001.
- [9] H. C. Liu, J. S. Min, and H. Samuelli, "A low-power baseband receiver IC for frequency-hopped spread spectrum communications," *IEEE Journal of Solid-State Circuits*, Vol. 31, No.3, pp. 384-394, March 1996.
- [10] C. Schurgers, O. Aberthorne, and M. B. Srivastava, "Modulation scaling for energy aware communication systems," *International Symposium on Low Power Electronics and Design*, pp. 96-99, 2001.
- [11] T. H. Lee, *The Design of CMOS Radio-Frequency Integrated Circuits*. Cambridge Univ. Press, Cambridge, U.K., 1998.
- [12] S. Cui, A. J. Goldsmith, and A. Bahai, "Modulation optimization under energy constraints," at *Proc. of ICC'03*, Alaska, U.S.A, May, 2003.
- [13] J. G. Proakis, *Digital Communications*, 4th Ed. New York: McGraw-Hill, 2000.
- [14] J. Cioffi, *Digital Communications*, EE379A Class Notes, Stanford University, Fall, 2001.
- [15] M. Steyaert, B. De Muer, P. Leroux, M. Borremans, and K. Mertens, "Low-voltage low-power CMOS-RF transceiver design," *IEEE Trans. Microwave Theory and Techniques*, vol. 50, pp. 281-287, January 2002.
- [16] S. Willingham, M. Perrott, B. Setterberg, A. Grzegorek, and B. McFarland, "An integrated 2.5GHz $\Sigma\Delta$ frequency synthesizer with 5 μ s settling and 2Mb/s closed loop modulation," *Proc. ISSCC 2000*, pp. 138-139, 2000.
- [17] P. J. Sullivan, B. A. Xavier, and W. H. Ku, "Low voltage performance of a microwave CMOS Gilbert cell mixer," *IEEE J. Solid-State Circuits*, vol. 32, pp. 1151-1155, July, 1997.
- [18] R. Min, A. Chadrakasan, "A framework for energy-scalable communication in high-density wireless networks," *International Symposium on Low Power Electronics Design*, 2002.
- [19] M. Gustavsson, J. J. Wikner, and N. N. Tan, *CMOS Data Converters for Communications*, Kluwer Academic Publishers, Boston, 2000.
- [20] E. Lauwers and G. Gielen, "Power estimation methods for analog circuits for architectural exploration of integrated systems," *IEEE Trans. VLSI System*, vol. 10, pp. 155-162, April, 2002.
- [21] S. Cui, A. J. Goldsmith, and A. Bahai, "Power estimation for Viterbi decoders," technical report, Wireless Systems Lab, Stanford University, 2003. Available at <http://wsl.stanford.edu/Publications.html>
- [22] T. Yamaji, N. Kanou, and T. Itakura, "A temperature-stable CMOS variable-gain amplifier with 80-dB linearly controlled gain range," *IEEE J. Solid-State Circuits*, vol. 37, pp. 553-558, May, 2002.
- [23] S. Cui, A. J. Goldsmith, and A. Bahai, "Joint Modulation and Multiple Access Optimization under Energy Constraints," to appear at *Globecom'04*, Dallas, Texas, U.S.A, December, 2004.
- [24] S. Boyd, L. Vandenberghe, *Convex Optimization*, Cambridge Univ. Press, Cambridge, U.K., 2003.



Shuguang Cui (S'99-M'05) received the B.Eng. degree in Radio Engineering with the highest distinction from Beijing University of Posts and Telecommunications, Beijing, China, in 1997, the M.Eng. degree in Electrical Engineering from McMaster University, Hamilton, Canada, in 2000, and the Ph.D. degree in Electrical Engineering from Stanford University, California, USA, in 2005. Since August of 2005, he has been working in the Department of Electrical and Computer Engineering at the University of Arizona as an Assistant Professor.

From 1997 to 1998 he worked at Hewlett-Packard, Beijing, P. R. China, as a system engineer. In the summer of 2003, he worked at National Semiconductor, Santa Clara, CA, as a wireless system researcher. His current research interests include cross-layer optimization for energy-constrained wireless networks, hardware and system synergies for high-performance wireless radios, and general communication theories. He is the winner of the NSERC graduate fellowship from the National Science and Engineering Research Council of Canada and the Canadian Wireless Telecommunications Association (CWTA) graduate scholarship.



Andrea J. Goldsmith (S'90-M'93-SM'99-F'05) is an associate professor of Electrical Engineering at Stanford University, and was previously an assistant professor of Electrical Engineering at Caltech. She has also held industry positions at Maxim Technologies and AT&T Bell Laboratories. Her research includes work on the capacity of wireless channels and networks, wireless communication and information theory, adaptive resource allocation in wireless networks, multi-antenna wireless systems, energy-constrained wireless communications, wireless communications for distributed control, and cross-layer design for cellular systems, ad-hoc wireless networks, and sensor networks. She received the B.S., M.S., and Ph.D. degrees in Electrical Engineering from U.C. Berkeley.

Dr. Goldsmith is a Fellow of the IEEE and of Stanford, and currently holds Stanford's Bredt Faculty Development Scholar Chair. She has received several awards for her research, including the National Academy of Engineering Gilbreth Lectureship, the Alfred P. Sloan Fellowship, the Stanford Terman Fellowship, the National Science Foundation CAREER Development Award, and the Office of Naval Research Young Investigator Award. She currently serves as editor for the Journal on Foundations and Trends in Communications and Information Theory and in Networks, and was previously an editor for the IEEE Transactions on Communications and for the IEEE Wireless Communications Magazine. Dr. Goldsmith is active in the IEEE Information Theory and Communications Societies and is an elected member of the Board of Governors for both societies.



Ahmad Bahai (S'91-M'93) received his MS degree from Imperial College, University of London in 1988 and Ph.D. degree from University of California at Berkeley in 1993, all in Electrical Engineering. From 1992 to 1994 he worked as a member of technical staff in the wireless communications division of TCSI Corporation, Berkeley, CA. He joined AT&T Bell Laboratories, Murray Hill, NJ, in 1994, where he was Technical Manager of Wireless Communication Group in Advanced Communications Technology Labs until 1997. He was involved in research

and design of several wireless standards such as Personal Digital Cellular (PDC), IS-95, GSM, and IS-136 terminals and Base stations, as well as ADSL and Cable modems. He is one of the inventors of Multi-carrier CDMA (OFDM) concept and proposed the technology for high speed wireless data systems. He was the co-founder and Chief Technical Officer of ALGOREX Inc., San Francisco, CA, and currently is a Fellow and the Chief Technologist of National Semiconductor, Santa Clara, CA. He is an adjunct/consulting professor at Stanford University and UC Berkeley. His research interest includes adaptive signal processing and communication theory. He is the author of more than 50 papers and reports. He is the author of Multi-carrier Digital Communications [Kluwer/Plenum, New York, 1999]. Dr. Bahai holds five patents in Communications and Signal Processing field and served as an editor of IEEE Communication Letters.